Electronic Supplementary Information for

Assembling Chirality into Magnetic Nanowires: Cyano-Bridged Iron(III)-Nickel(II) Chains Exhibiting Slow Magnetization Relaxation and Ferroelectricity

Cai-Feng Wang, Dong-Ping Li, Xin Chen, Xiao-Ming Li, Yi-Zhi Li, Jing-Lin Zuo* and Xiao-Zeng You

State Key Laboratory of Coordination Chemistry, School of Chemistry and Chemical Engineering, Nanjing National Laboratory of Microstructures, Nanjing University, Nanjing 210093, P. R. China

Index Page

Experimental Section

General considerations. All chemicals were reagent grade and used as received. (1*S*,2*S*)-(+)-1,2-diaminocyclohexane and (1*R*,2*R*)-(–)-1,2-diaminocyclohexane were purchased form the Aldrich Chemicals Company. $(Bu_4N)[(Tp)Fe(CN)_3]$ was prepared according to the literature method (See: R. Lescouëzec, J. Vaissermann, F. Lloret, M. Julve, M. Verdaguer, *Inorg. Chem*. 2002, **41**, 5943). While no problems were encountered in this work, cyanides are toxic and perchlorate salts are potentially explosive. Thus, these starting materials should be handled in small quantities and with great caution!

$\{[(Tp)_2Fe_2(CN)_6Ni_3((1S,2S)\text{-chxn})_6](ClO_4)_4\cdot 2H_2O\}_n$ (1). A solution of (1*S*,2*S*)-chxn (34.3 mg, 0.3 mmol) in water (2 mL) was added dropwise to a solution of $Ni(ClO_4)_2\cdot 6H_2O$ (54.9 mg 0.15 mmol) in acetonitrile (8 mL), resulting in the formation of a purple solution. Treatment of this mixture with a solution of $(Bu_4N)[(Tp)Fe(CN)_3]$ (59.1 mg, 0.1 mmol) in methanol (20 mL) afforded an orange solution. Red-brown plate-like crystals were obtained by slow evaporation of the resulting solution in air after about one month. Yield: 45.7 mg, 46%. Anal. Calcd for $C_{60}H_{108}B_2Cl_4Fe_2N_{30}Ni_3O_{18}$: C 36.23, H 5.47, N 21.13; found: C 36.31, H 5.50, N 21.09. IR (KBr, cm^{-1}): ν_{CN} = 2153 (m), 2125 (w).

$\{[(Tp)_2Fe_2(CN)_6Ni_3((1R,2R)\text{-chxn})_6](ClO_4)_4\cdot 2H_2O\}_n$ (2). Red-brown plate-like crystals of complex **2** were prepared as described above for **1**, except that (1*R*,2*R*)-chxn was used. Yield: 41.8 mg, 42%. Anal. Calcd for $C_{60}H_{108}B_2Cl_4Fe_2N_{30}Ni_3O_{18}$: C 36.23, H 5.47, N 21.13; found: C 36.35, H 5.43, N 20.97. IR (KBr, cm^{-1}): ν_{CN} = 2153 (m), 2125 (w).

X-ray Crystallography. The crystal structures were determined on a Siemens (Bruker) SMART CCD diffractometer using monochromated Mo-$K\alpha$ radiation (λ = 0.71073 Å) at room temperature. Cell parameters were retrieved using SMART software and refined using SAINT on all observed reflections. Data were collected using a narrow-frame method with scan widths of 0.30° in ω and an exposure time of 10 s / frame. The highly redundant data sets were reduced using SAINT and corrected

for Lorentz and polarization effects. Absorption corrections were applied using SADABS supplied by Bruker. Structures were solved by direct methods using the program SHELXL-97. The positions of the metal atoms and their first coordination spheres were located from direct-method *E* maps; other non-hydrogen atoms were found using alternating difference Fourier syntheses and least-squared refinement cycles and, during the final cycles, were refined anisotropically. Hydrogen atoms were placed in calculated position and refined as riding atoms with a uniform value of U_{iso}.

Physical Measurements. Elemental analyses for C, H and N were performed on a CHN-O-Rapid analyzer and an Elementar Vario MICRO analyzer. Infrared spectra were recorded on a Vector22 Bruker spectrophotometer with KBr pellets in the 400–4000 cm^{-1} region. The circular dichroism spectra were recorded on a JASCO J–810 Spectropolarimeter with KBr pellets. A pulsed Q-switched Nd:YAG laser at a wavelength of 1064 nm was used to generate SHG signal. Magnetic susceptibility measurements were obtained with the use of a Quantum Design MPMS-XL7 SQUID magnetometer at temperatures ranging from 1.8 to 300 K. The DC measurements were collected using applied fields in the range 0–7 T. Data were corrected for diamagnetic contributions calculated from Pascal constants. The AC measurements were performed at various frequencies from 1 to 1488 Hz with the AC field amplitude of 5 Oe and no DC field applied. Ferroelectric property in a pellet of powder samples was measured by the Premier II ferroelectric tester at room temperature.

Table S1. Selected bond lengths(Å) and angles (°) in complexes **1** and **2** .

Complex 1					
Fe1–N1	1.845(6)	Fe1–N3	1.990(5)	Fe1–N5	1.886(7)
C19–Fe1	1.919(8)	C20–Fe1	2.085(6)	C21–Fe1	2.064(7)
Fe2–N7	2.141(7)	Fe2–N9	1.880(5)	Fe2–N11	2.093(5)
C22–Fe2	1.860(7)	C23–Fe2	1.953(8)	C24–Fe2	1.826(5)
N14–Ni1	2.041(5)	N17^{a}–Ni1	2.007(6)	N19–Ni1	2.410(5)
N20–Ni1	2.130(5)	N21–Ni1	2.078(5)	N22–Ni1	2.164(5)
N15–Ni2	2.166(6)	N16–Ni2	2.136(5)	N23–Ni2	2.134(5)
N24–Ni2	2.085(5)	N25–Ni2	2.120(5)	N26–Ni2	2.117(5)
N13–Ni3	2.108(7)	N18^{a}–Ni3	2.110(5)	N27–Ni3	2.095(5)
N28–Ni3	2.239(4)	N29–Ni3	2.139(5)	N30–Ni3	2.350(5)
C20–N14	1.079(6)	C21–N15	1.132(7)	C22–N16	1.143(7)
C19–N13	1.114(7)	N3–Fe1–C20	170.94(18)	N14–C20–Fe1	156.3(5)
C20–N14–Ni1	176.4(5)	N14–Ni1–N21	145.6(2)	N1–Fe1–C21	170.65(17)
N15–C21–Fe1	169.6(5)	C21–N15–Ni2	142.2(4)	N16–Ni2–N15	169.51(19)
C22–N16–Ni2	167.2(4)	N16–C22–Fe2	165.8(4)	C22–Fe2–N11	170.6(2)
N13–Ni3–N30	146.21(18)	C19–N13–Ni3	165.1(5)	N13–C19–Fe1	171.5(5)
N5–Fe1–C19	174.15(19)	C23^{a}–N17^{a}–Ni1	157.3(4)	C24^{a}–N18^{a}–Ni3	161.9(4)
N17–C23–Fe2	167.7(5)	N18–C24–Fe2	177.3(4)	N21–Ni1–N22	80.2(2)
Complex 2					
Fe1–N1	1.831(7)	Fe1–N3	1.973(7)	Fe1–N5	1.895(7)
C55–Fe1	1.949(8)	C56–Fe1	2.047(7)	C57–Fe1	2.061(7)
Fe2–N7	2.108(7)	Fe2–N9	1.904(6)	Fe2–N11	2.097(6)
C58–Fe2	1.856(8)	C59–Fe2	1.936(8)	C60–Fe2	1.876(7)
N13–Ni1	2.174(6)	N14–Ni1	2.179(5)	N15–Ni1	2.159(5)
N16–Ni1	2.132(6)	N25–Ni1	2.079(7)	Ni1–N30^{a}	2.101(6)
N17–Ni2	2.283(6)	N18–Ni2	2.134(5)	N19–Ni2	2.092(5)
N20–Ni2	2.078(5)	N27–Ni2	2.133(6)	N28–Ni2	2.120(7)
N21–Ni3	2.096(7)	N22–Ni3	2.081(6)	N23–Ni3	2.185(5)
N24–Ni3	1.998(7)	N26–Ni3	2.030(6)	N29^{a}–Ni3	2.073(7)
C55–N25	1.118(8)	C57–N27	1.119(7)	C58–N28	1.168(8)
C56–N26	1.110(7)	N5–Fe1–C55	176.3(2)	N25–C55–Fe1	169.8(6)
C55–N25–Ni1	169.5(5)	N25–Ni1–N15	153.6(2)	N1–Fe1–C57	172.5(2)
N27–C57–Fe1	173.2(6)	C57–N27–Ni2	144.2(4)	N28–Ni2–N27	172.5(2)
N28–C58–Fe2	167.9(6)	C58–N28–Ni2	166.4(4)	C58–Fe2–N11	171.6(2)
N3–Fe1–C56	171.9(2)	N26–C56–Fe1	158.3(6)	C56–N26–Ni3	176.4(7)
N26–Ni3–N23	151.4(3)	C60^{a}–N30^{a}–Ni1	161.2(4)	C59^{a}–N29^{a}–Ni3	156.8(5)

^{a} Symmetry transformation used to generate equivalent atoms: x, y−1, z.

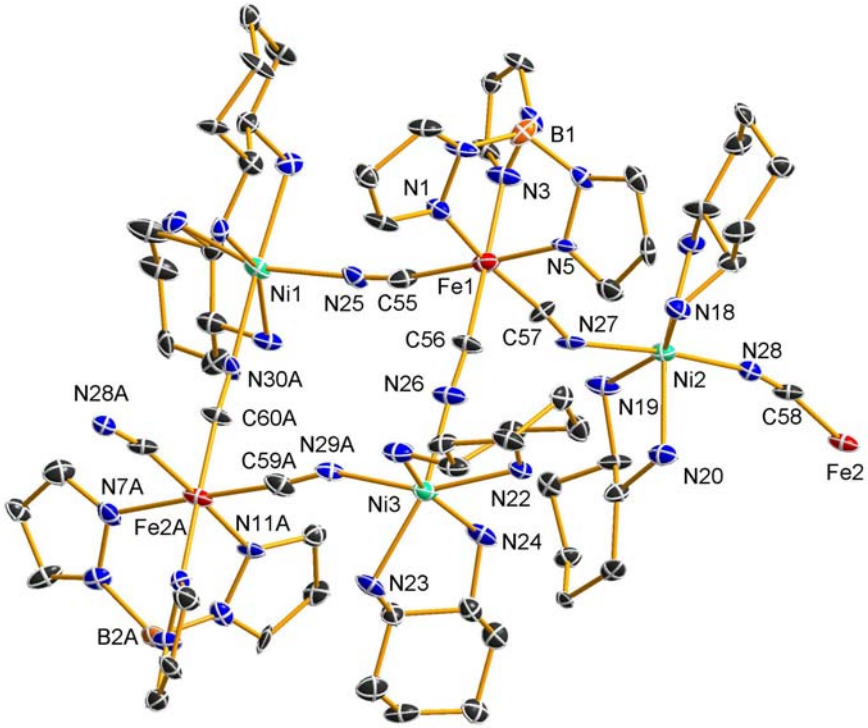

Fig. S1 Asymmetric strucutural unit of **2**; hydrogen atoms, perchlorate anions and noncoordinated crystalline water molecules are omitted for clarity (ORTEP, 30% ellipsoids).

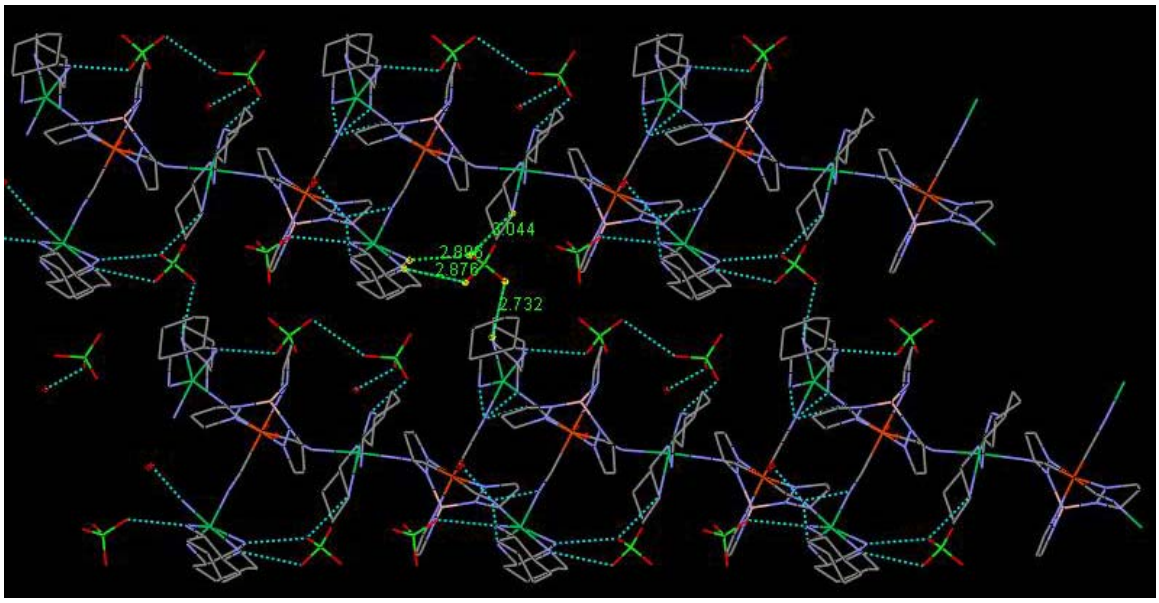

Fig. S2 The layer structure of complex **1** runs along the *bc* plane created by hydrogen bonds (2.896 Å for N22···O31, 3.044 Å for N23···O31, 2.876 Å for N19···O34, and 2.732 Å for N30···O33).

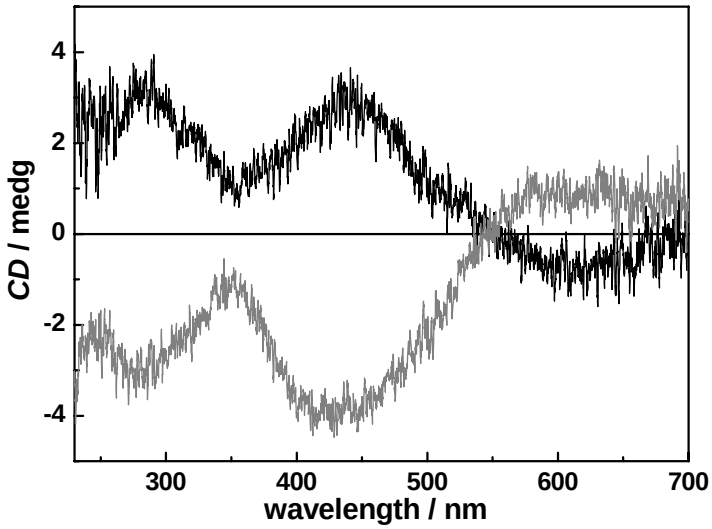

Fig. S3 Circular dichroism spectra of **1** (*S* isomer, black) and **2** (*R* isomer, gray) in KBr pellets.

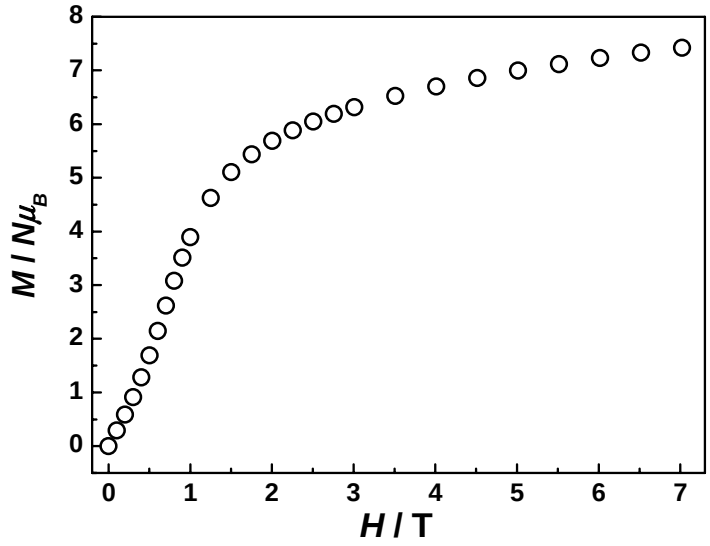

Fig. S4 Field dependence of magnetization for **1** measured at 1.8 K.

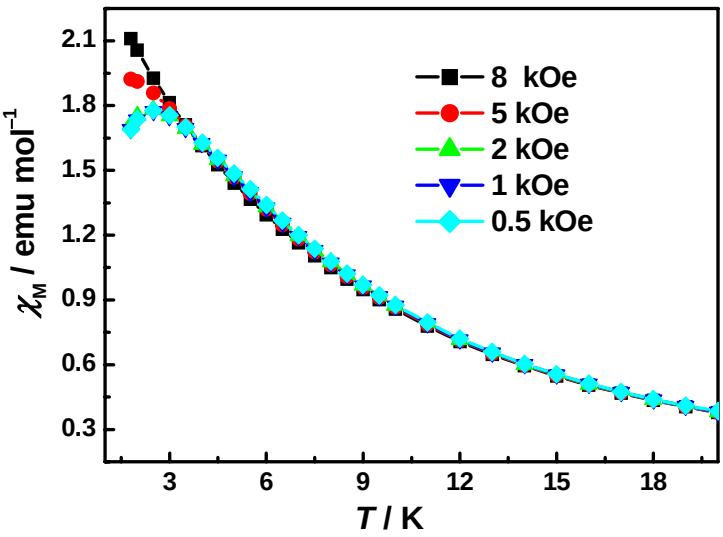

Fig. S5 Field dependence of the magnetic susceptibility of **1** at very low temperatures. The solid line is simply to guide the eye.

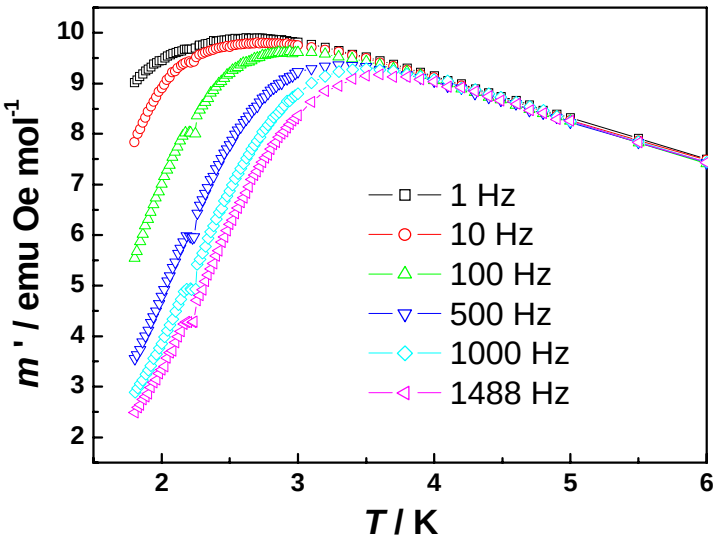

Fig. S6 Frequency dependence of the in-phase *m*′ component versus *T* for **1** in a 5 Oe AC field oscillating at frequencies between 1 and 1488 Hz under a zero DC field.

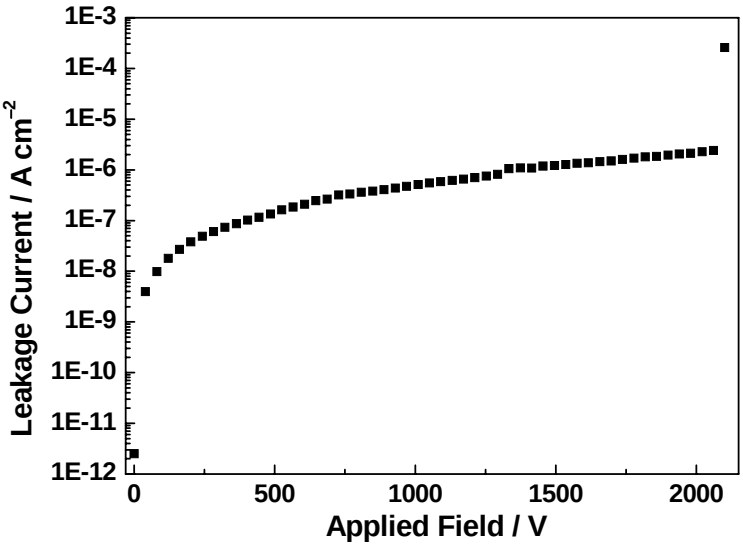

Fig. S7 Plot of leakage currents versus electric fields for **1**.

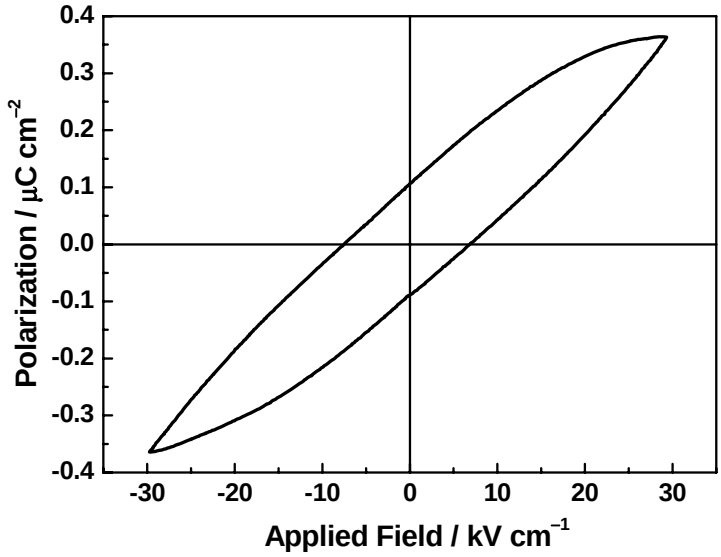

Fig. S8 Polarization versus applied electric field curve of **2** at room temperature.